J. Fluid Mech. (1988), *vol.* 196, *pp.* 135–156
Printed in Great Britain

The dynamics and structure of double-diffusive layers in sidewall-heating experiments

By J. TANNY† AND A. B. TSINOBER‡

†Center for Technological Education, Holon, P.O. Box 305, Holon, Israel

‡Department of Fluid Mechanics and Heat Transfer, Faculty of Engineering, Tel-Aviv University, Tel-Aviv, Israel

(Received 13 May 1987 and in revised form 10 March 1988)

The dynamics and structure of double-diffusive layers were studied experimentally by heating a linear stable solute gradient from a sidewall in a wide tank. The formation and subsequent development of the layers were investigated by various flow-visualization techniques, namely fluorescent dye, fluorescent particles and shadowgraph. Experiments were performed in order to determine the stability diagram of the flow, following in each experiment the phase trajectory of the system in the phase plane of thermal and solute Rayleigh numbers. The experimentally obtained stability diagram appears to be similar to that obtained numerically by Thangam *et al.* (1981) and by Hart (1971) for a vertical narrow slot and a steady basic flow. It is shown that if the temperature of the sidewall rises slowly to its prescribed value, the thickness of the initial layers, formed at the onset of instability, is a function of the ambient density gradient and fluid properties only. On the other hand, if the wall temperature rises quickly (almost impulsive heating), the thickness of the initial layers is proportional to the imposed temperature difference, provided that the Rayleigh number, based on this difference, is larger than some critical value which is associated with the first merging of the layers. A criterion for the first merging of the initial layers is obtained, and it is suggested that this merging is due to subsequent instability of the system. The subsequent merging process, following the first merging, is not a simple successive doubling of the layer thickness and in each of five nearly identical experiments a different dependence of the average layer thickness on the instantaneous Rayleigh number is obtained. This indicates that the system of layers behaves chaotically after the first merging. The final thickness of the layers depends on the prescribed lateral temperature difference, and the ratio between the final and the initial thickness of the layers is a linear function of the final Rayleigh number. Flow-visualization experiments indicate that the layers consist of vortices with vertical scale of the layer thickness and various horizontal scales.

1. Introduction

Double-diffusive convection may arise in a fluid that contains opposing gradients of two buoyancy components with different molecular diffusivities. Although the fluid is initially statically stable, in certain conditions the potential energy stored in the component distributed unstably may be released, giving rise to convective motions (for reviews see Turner 1974, 1979, 1985; Huppert & Turner 1981).

One of the basic phenomena in double-diffusive convection is the splitting of a smooth statically stable solute gradient into a system of horizontal layers due to these convective motions. For example, when a linear stable solute gradient is heated

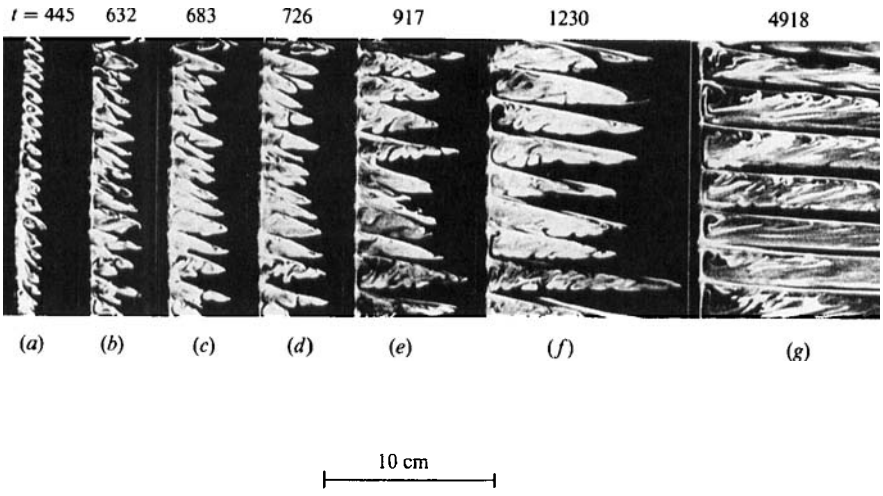

FIGURE 1. The formation and development of layers in a linear solute gradient subjected to heating from a vertical sidewall. (*a*) Initial layers; (*b–f*) merging process; (*g*) final layers (fragment).

from a vertical sidewall, and the Rayleigh number based on the lateral temperature difference between the wall and the ambient fluid is larger than some critical value, instability takes place in the form of a system of roll-cells, formed simultaneously along the heated wall. These cells grow laterally and ultimately produce the layered system (figure 1). For the case of a wide container, which is our main interest in this work, the corresponding critical Rayleigh number $Ra_{\eta cr}$, was found by Chen, Briggs & Wirtz (1971) to be $Ra_{\eta cr} = 1.5 \times 10^4$. Here $Ra_\eta = g\alpha \Delta T' \eta^3 / \nu K_T$, where g is the gravitational acceleration, α is the coefficient of thermal expansion, $\Delta T'$ is the horizontal temperature difference between the wall and the ambient fluid, ν is the kinematic viscosity, K_T is the thermal diffusivity and $\eta = \alpha \Delta T / \phi_0$ where $\phi_0 = -\beta \, \mathrm{d}s_0/\mathrm{d}z$, β being the coefficient of solutal expansion and $\mathrm{d}s_0/\mathrm{d}z$ is the ambient solute gradient. The subscript cr denotes critical state. Chen *et al.* also found that the thickness of the layers, h, was equal to $(0.67\text{–}0.97)\,\eta$, with an average of 0.8η for Ra_η ranging from 14000 to 54000. They concluded that the lengthscale η was a proper choice for the layers thickness. Wirtz, Briggs & Chen (1972) investigated the same problem numerically and experimentally and obtained essentially the same results. They also conducted salinity and temperature measurements within the developed layers and showed that the fluid in the layers is well mixed and the layers are separated by sharp interfaces with large salinity and temperature gradients across them. Huppert & Turner (1980) carried out an extensive study of this case for Rayleigh numbers up to 4.4×10^9 and concluded that for $Ra_\eta > 2 \times 10^5$ the thickness of the layers, h, expressed as a fraction of η is essentially constant and close to 0.6η. They also found that as the Rayleigh number increases from its critical value up to 2×10^5, h/η steadily falls from unity to about 0.6. Huppert, Kerr & Hallworth (1984) showed that these results hold for other values of the Prandtl number $Pr = \nu/K_T$ and the diffusivity ratio $\tau = K_S/K_T$, where K_S is the solutal diffusivity.

It is noteworthy that in the experiments mentioned above the temperature of the wall was kept constant with time except for a transient period between the moment when the heat was turned on and the moment when the wall temperature reached the prescribed value. Only Chen *et al.* (1971) reported a time constant, t_0, of about

180 s for the rising curve of the temperature of the heated wall in the normalized form:

$$\Delta T = 1 - \exp\left(-\frac{t}{t_0}\right), \tag{1}$$

where t is the time measured from initiation of heating. Huppert & Turner (1980) and Huppert *et al.* (1984) did not specify the time constant, t_0, but it is assumed here to be of the same order of magnitude due to similar experimental procedures.

The case of a linear stable solute gradient heated from a sidewall by a uniform heat flux was studied by Narusawa & Suzukawa (1981) and by Suzukawa & Narusawa (1982). They showed the existence of a critical non-dimensional heat flux below which no layers occurred at all even up to temperature differences corresponding to Ra_η as high as 10^6. This result indicates the importance of the transient period in the temperature-rise curve (1) for the formation and development of layers in experiments with constant wall temperature. Suzukawa & Narusawa (1982) investigated the structure of the layers by temperature measurements within the layers. They showed that the propagation velocity of the fronts of the layers was constant with time and increased with increasing heat flux at the wall. The layers were separated by sharp interfaces with relatively large temperature differences across them.

A related configuration of interest is that of a linear stable solute gradient heated differentially in a vertical narrow slot. It should be emphasized that the basic flow in this case is steady while the basic flow in the case of a wide container is unsteady.

Thorpe, Hutt & Soulsby (1969) carried out a linear stability analysis for the narrow-slot configuration and found that for large values of the solute Rayleigh number, Ra_S, the critical thermal Rayleigh number is $Ra_{T\mathrm{cr}} = 2.76 Ra_S^{\frac{5}{8}}$. Here $Ra_T = g\alpha \Delta T d^3/\pi^4 \nu K_S$ and $Ra_S = g\phi_0 d^4/\pi^4 \nu K_S$, where d is the width of the slot. They also found that the thickness of the initial cells was $h = d(2/Ra_S)^{\frac{1}{6}}$, and they rotated with alternating senses. Their experimental results were in fairly good agreement with the theory provided that the measured initial thickness was compared to twice the predicted one. This was due to the merging of the counter-rotating pairs of cells which was assumed to occur at the very early stages of the experiment.

Hart (1971, 1973) investigated the same case numerically and took proper account of both the mean field and the boundary conditions. The results he obtained were in somewhat better agreement with the experimental results of Thorpe *et al.* (1969) than their theoretical results. The stability curve presented by Hart (1971) indicated transition from shear to double-diffusive instability as the solute gradient increased from zero to some specific value. In particular, as Ra_S increased slightly above 10^3, the critical Ra_T decreased sharply from 10^5 to about 2×10^2. Here, K_T and not K_S appears in the denominator of Ra_T. This sharp decrease in Ra_T exhibited the destabilizing effect of the solute gradient. Thangam, Zebib & Chen (1981) studied this flow in more detail and obtained essentially the same results.

In all the above-mentioned works, no detailed study of the merging process of the layers was carried out, and the merging process was examined only qualitatively.

Linden (1976) examined the process of destruction of interfaces in the case of a stable density gradient subjected to a uniform buoyancy flux from above. He indicated two mechanisms for layers merging: (i) vertical migration of the interface separating the layers, and (ii) the breakdown of that interface. Huppert & Linden (1979) observed merging of layers when a stable salinity gradient was heated uniformly from below. Most of the merging they observed occurred owing to the

breakdown of the interfaces separating the layers. Their measurements showed that merging of two adjacent layers is a result of the equalization of their densities. Turner & Chen (1974) considered two-dimensional effects in double-diffusive convection and observed a wavy-like interface that was produced as a result of merging occurring at different rates at different horizontal positions. Hart (1973) considered merging of layers in the narrow-slot case and observed that it occurred owing to the breakdown of interfaces 'in a shower of turbulence and salt fingers'. Wirtz & Reddy (1979) studied in more detail the merging of layers in the narrow-slot configuration and as a result concluded that the merging process takes place by successive doubling of the layers thickness.

The aim of this work was to study the dynamics and structure of double-diffusive layers in sidewall heating experiments in a wide tank in which we expect qualitatively different behaviour of the system from that in the narrow-slot configuration. In particular the following questions were addressed: (1) What is the criterion for onset of layers, what is their initial thickness and how are these parameters influenced by the transient period of heating? (ii) What are the characteristics of the merging process of the layers? (iii) What is the structure of the initial and developed layers and interfaces? This introduction is followed by §2 where some qualitative considerations which predict part of the experimental results are presented. In §3, the experimental apparatus and techniques are described; in §4, the results are presented and discussed and the concluding remarks are in §5. Part of the material in this paper was presented in Tsinober & Tanny (1985, 1986) and Tanny & Tsinober (1987).

2. Qualitative considerations and dimensional analysis

2.1. *The initial thickness of the layers*

Chen *et al.* (1971) showed that when a linear stable salt gradient is heated from a sidewall, layers start to form at a critical Rayleigh number:

$$Ra_{\eta \mathrm{cr}} = \frac{g\alpha \Delta T' \eta^3}{\nu K_T} = 1.5 \times 10^4, \tag{2}$$

and the thickness of the layers at their onset and at Rayleigh numbers close to the critical is defined by

$$h_{\mathrm{i}} = 0.83\alpha \Delta T/\phi_0. \tag{3}$$

The coefficient 0.83 is an average of experiments no. 6 and 11, from Chen *et al.* (1971, table 1) for Rayleigh numbers 14200 and 18000 respectively, which are closest to the critical one.

From (2) and (3) one obtains

$$h_{\mathrm{i}} = 9.2\left(\frac{\nu K_T}{g\phi_0}\right)^{\frac{1}{4}}. \tag{4}$$

This result means that in fact the initial thickness of the layers depends on the ambient solute gradient and fluid properties only. In the following we shall use a different form of relation (4):

$$h_{\mathrm{i}} = 9.2\left(\frac{\nu K_S}{g\phi_0}\right)^{\frac{1}{4}} \quad \tau^{-\frac{1}{4}} = 29.1\xi. \tag{5}$$

The lengthscale $\xi = (\nu K_S/g\phi_0)^{\frac{1}{4}}$ can also be obtained by simple dimensional analysis if one looks for a lengthscale independent of ΔT. The choice of νK_S in the definition of ξ, rather than νK_T or $K_S K_T$ will be justified later, in view of the experimental results obtained.

2.2. *The merging process*

It is noteworthy that h_i is the thickness of the initial layers formed at the onset of instability ($Ra_\eta = Ra_{\eta cr}$), and it is assumed that although the lateral temperature difference (and Ra_η) further increase, this thickness is preserved for some period of time, at least for Rayleigh numbers just slightly exceeding the critical one. At some higher Rayleigh number the layers will merge, increasing their thickness. Since for large Rayleigh numbers the layer thickness is defined by η and the initial thickness of the layers is defined by ξ, one can obtain the ratio:

$$\frac{h_f}{h_i} = \frac{0.6\eta}{29.1\xi} = 0.02 Ra_\xi, \tag{6}$$

where h_f is the final thickness of the layers. The parameter Ra_ξ is a Rayleigh number based on ξ, and is related to Ra_η and τ by:

$$Ra_\xi = \left(\frac{Ra_\eta}{\tau}\right)^{\frac{1}{4}} = \frac{g\alpha\,\Delta T\,\xi^3}{\nu K_S}. \tag{7}$$

The consequence of (6) is that the ratio between the final thickness of the layers, h_f, and their initial thickness, h_i, can assume any value depending on Ra_ξ and generally it is not equal to 2^n (n is a non-negative integer) as it would have been if the initial thickness of the layers was doubled successively. Therefore one can expect much more complex behaviour of the system of layers in the case of the wide gap than in the case of the narrow slot for which Wirtz & Reddy (1979) showed that merging occurs as successive doubling of the layers thickness.

3. Apparatus and experimental techniques

Two different pieces of experimental apparatus were used: one with a large tank and one with a small tank. Most of the experiments were conducted in a large Perspex tank (50 × 120 × 50 cm high) with one sidewall (50 × 50 cm) made of a 3 mm brass plate (figure 2). Behind that plate was a series of 36 cylindrical heating elements, operated by an electric variable-power source. The other three walls of the tank were insulated by special transparent thermal insulation units, each of them consisted of four thin (1.5 mm thick) Perspex plates separated by 3 mm air gaps. This special insulation allowed continuous illumination and flow visualization throughout the experiment. The vertical linear solute gradient was established by a standard 'double bucket' system using salt, sugar and glycerol solutions. The horizontal temperature difference was measured by thermocouples type T with accuracy of ± 0.3 °C. Thirteen thermocouples were distributed at the vertical centreline of the brass plate and two in the ambient fluid. Another thermocouple was mounted on a probe that was traversed vertically to measure temperatures inside the body of the layers. The output of the thermocouples was measured and linearized by a data logger. A specially designed feedback and control system included the power source, the data logger and a VAX-750 computer. This system allowed the wall temperature to rise to a prescribed value following relation (1) with different value of t_0 in each experiment, and afterwards maintained the wall at this temperature throughout the rest of the experiment.

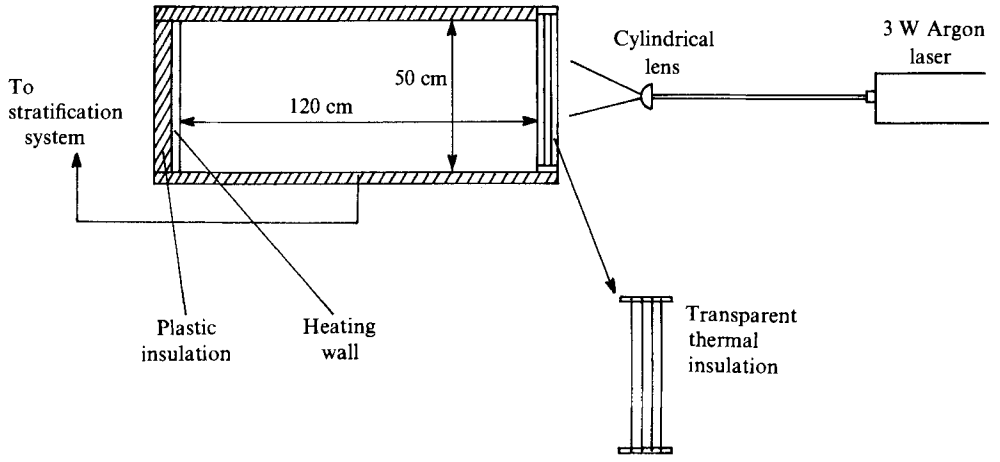

FIGURE 2. A schematic side view of the experimental apparatus (large tank).

The formation, merging and development of the layers were visualized using a tracer dye visualization. The fluid near the wall was tagged by dropping a particle of a fluorescent dye (Rhodamine B) and was illuminated by a 1 mm thick vertical sheet of light produced by a 3W argon laser. The formation, merging and subsequent development of the layers were photographed, a typical set of photographs is shown in figure 1. The average thickness of the layers was measured from the photographs by counting the number of layers in a known distance along the wall. The thickness of the layers was always measured at the wall because it is the wall temperature to which it is related. This should be kept in mind because usually the merging of two adjacent layers starts at the wall and then propagates into the fluid so that in fact the average thickness of the layers is, in some circumstances, a function of the distance from the wall. In some typical experiments the individual thickness of the layers was also measured in order to estimate σ, the standard deviation from the average layer thickness.

The shadowgraph technique was also used either simultaneously or separately as a cross-check for the determination of the stability diagram of the flow.

The structure of the layers was studied, in part, by a different visualization technique, using small particles (≈ 4 μm in diameter) dyed with a yellow fluorescent dye. The fluorescence was excited by operating the laser in the blue line (488 nm). The photographs were taken through a yellow optical filter in order to enhance the contrast between the particles traces and the background.

Part of the results concerning the initial thickness of the layers, their first merging and their structure were taken from experiments conducted in the small tank. This tank ($34 \times 40 \times 28$ cm high) operated in the same manner as the large tank, the only difference being that the heating of the sidewall was carried out by circulating preheated water in a small container at the back of the brass plate. In this tank three types of experiments were conducted. In the first type ΔT was raised according to relation (1). In the second type ΔT was raised almost impulsively also following relation (1) but with very small t_0 in the range 1.3–4 s. This was carried out by pouring preheated water into the small container behind the plate. In the third type, ΔT was raised linearly with time.

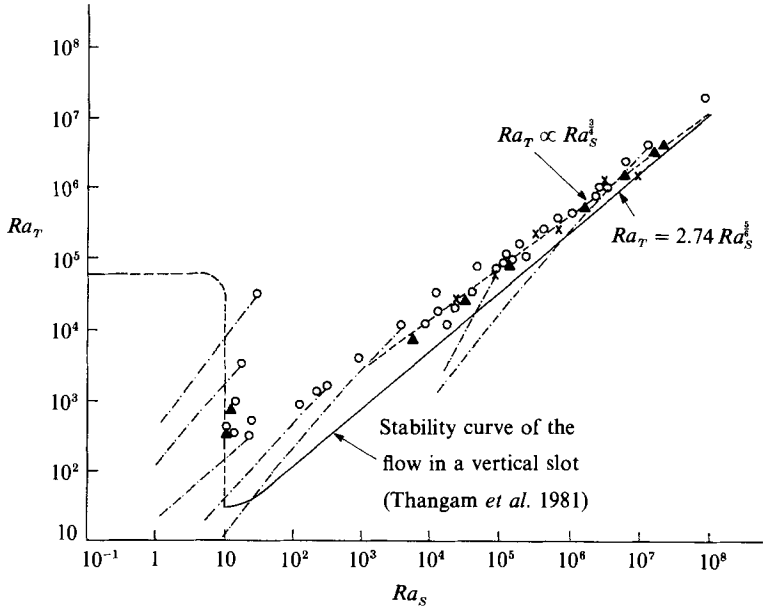

FIGURE 3. The stability diagram. The symbols corrrespond to the present experimental results: ○, $\Delta T = 1-\exp(-t/t_0)$, salt; ▲, $\Delta T = 1-\exp(-t/t_0)$, sugar; ×, $\Delta T = ct$, salt. —·—, phase trajectories.

4. Results and discussion

4.1. *Experimental stability analysis*

The stability analysis was focused on two main issues: (i) determination of criterion for onset of instability; and (ii) determination of the thickness of the layers formed at the moment of instability.

The experimental results for salt and sugar gradients from experiments in which ΔT was raised according to relation (1) with $t_0 = 75$–8000 s and from experiments with a linear relation between ΔT and time (conducted in the small tank) are shown in figure 3 along with the numerical stability curve of the flow in a vertical narrow slot obtained by Thangam *et al.* (1981). Since in the present semi-infinite configuration there is no external lengthscale as in the case of the narrow slot, Ra_T and Ra_S are based on the heat conduction characteristic length, $\delta = (K_T t)^{\frac{1}{2}}$, where t is the time measured from the initiation of heating. Here, $Ra_T = g\alpha\,\Delta T\,\delta^3/\nu K_T$ and $Ra_S = g\phi_0\,\delta^4/\nu K_T$. All the data points in the figure represent critical values of Ra_T and Ra_S at the moment of instability onset ($t = t_{\rm cr}$, $\delta = \delta_{\rm cr}$) and for some typical experiments, the phase trajectory is also plotted. This trajectory represents the path of the system as a function of time in the (Ra_T, Ra_S)-plane before instability takes place ($t < t_{\rm cr}$), and is terminated by a data point.

We chose to represent the results of the stability analysis in the phase plane since it allows one to regard the unsteady basic state in the semi-infinite configuration as a set of successive approximate 'frozen' steady states. Thus a direct comparison with the stability of the flow in the narrow-slot configuration is possible.

It is seen from the figure that the stability curve in the present semi-infinite configuration is essentially the same as that for the vertical narrow slot. The

consequence of this result is that the nature of the instability is similar in the two configurations in spite of the fact that in the narrow slot the basic state is steady while here it is unsteady. The general agreement between the two results may be due to the similarity of the velocity profile in the two cases. As was shown by Paliwal & Chen (1980) the steady-state velocity profile in the narrow-slot case becomes zero at $x \approx 0.1d$. This means that from that point of view, the narrow slot is in fact a 'wide' slot.

The difference between the results of the two cases is mainly quantitative. For $Ra_S > 10^3$ the slope of the curve for the narrow slot is 5/6 while for the large tank a least-squares fit to the data gives a slope of 3/4. If we assume that this slope represents the instability behaviour, we can write $Ra_{T\mathrm{cr}} \propto Ra_S^{\frac{3}{4}}$, i.e. $g\alpha\,\Delta T_{\mathrm{cr}}\,\delta_{\mathrm{cr}}^3/\nu K_T \propto (g\phi_0\,\delta_{\mathrm{cr}}^4/\nu K_T)^{\frac{3}{4}}$, or

$$\frac{g\alpha\,\Delta T_{\mathrm{cr}}}{\nu K_T}\left(\frac{\nu K_T}{g\phi_0}\right)^{\frac{3}{4}} = \text{constant}. \tag{8}$$

Replacing K_T by K_S one obtains eventually

$$Ra_{\xi\mathrm{cr}} = \text{constant}. \tag{9}$$

Thus within the accuracy of our measurements, $Ra_{\xi\mathrm{cr}}$ is constant and independent of t_0, which was varied in this range of the curve ($Ra_S > 10^3$) from 200 to 8000 s. The average value of $Ra_{\xi\mathrm{cr}}$ from 36 data points with $Ra_S > 10^3$ is 53.8 ± 12. This result is somewhat higher than $Ra_{\xi\mathrm{cr}} = 35 \pm 4$ obtained by Chen *et al.* (1971) for $t_0 = 180$ s. It should be noted that the present results are from experiments conducted in the small (34 cm wide) and in the large (120 cm wide) tanks, while Chen *et al.* conducted their experiments in a tank of only 12.5 cm width. It is possible that the relatively narrow tank they used affected their results slightly.

It is noteworthy that the results from experiments with a linear relation between wall temperature and time do not deviate significantly from the other results. Thus it is concluded that for the two heating types considered, the instability of the system is insensitive to the character of the temperature-rise curve.

The result that for large Ra_S ($> 10^3$), $Ra_{\xi\mathrm{cr}}$ is independent of t_0 is in some contradiction to the result obtained by Narusawa & Suzukawa (1981) for the case of constant heat flux at the wall. In particular they showed that for very low non-dimensional heat flux at the wall (corresponding to very large t_0 in our experiments), no layers were formed at all even for $Ra_\eta = 6 \times 10^5$ ($Ra_\xi = 88$), which is much larger than the critical one. Their result means that in our case, $Ra_{\xi\mathrm{cr}}$ should depend on t_0. A possible answer to this discrepancy is that our experimental results in figure 3 may represent a line with a slope slightly larger than 3/4, for example, 5/6. If this is so, the stability curve is $Ra_{\xi\mathrm{cr}} = \text{constant} \times Ra_S^{\frac{1}{12}}$ and not $Ra_{\xi\mathrm{cr}} = \text{constant}$. Since Ra_S increases with t_{cr} and for a given solute gradient t_{cr} increases with t_0, a very weak dependence of $Ra_{\xi\mathrm{cr}}$ on t_0 is obtained and a stable flow is possible even for very large Ra_ξ provided the heating is very slow. To explore the exact slope of the stability curve, very accurate experiments in a very wide range of Ra_S are needed. However, since no other conclusive results are available, it is concluded on the basis of the present results that the slope of the stability curve, in the range of Ra_S investigated, is 3/4 and that $Ra_{\xi\mathrm{cr}} = \text{constant}$.

At small values of Ra_S ($10 < Ra_S < 10^2$) there is a more significant deviation of the experimental results from the theoretical curve for the narrow slot, but still the results represent the destabilization of the basic flow as Ra_S is increased slightly above some critical value. It should be noted that it was very difficult to obtain

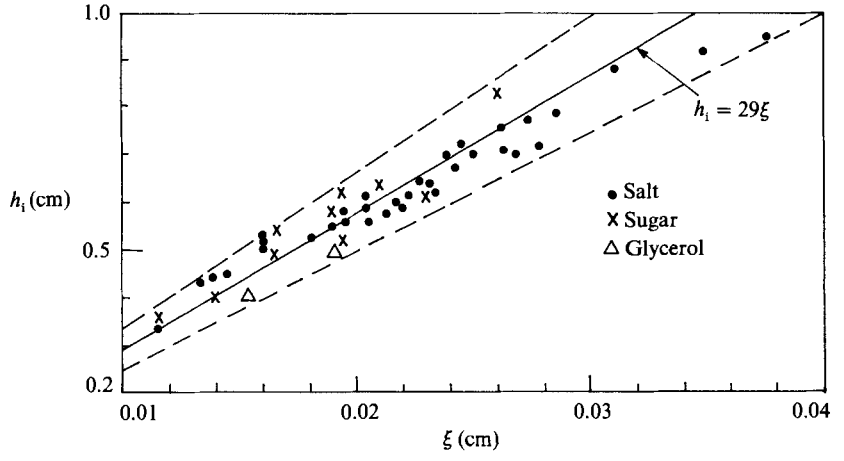

FIGURE 4. The dependence of the initial thickness of the layers, h_i, on the lengthscale ξ.

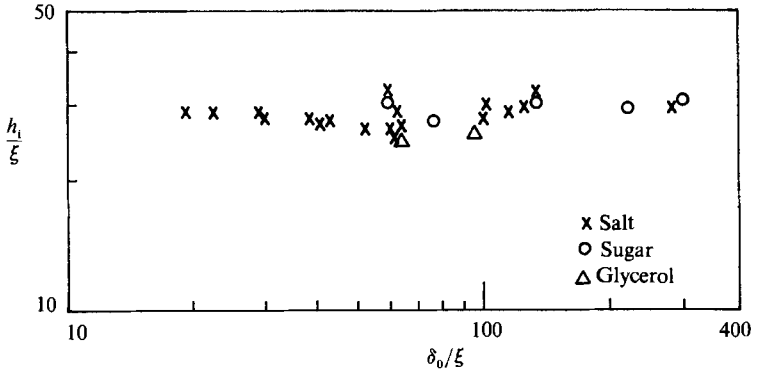

FIGURE 5. The dependence of the non-dimensional initial thickness of the layers, h_i/ξ, on the non-dimensional lengthscale δ_0/ξ.

accurate results in this range owing to the very small solute gradients needed and/or very small t_0. Therefore, the determination of the moment of instability (t_{cr}) in this range was less accurate ($\pm 30\%$), which resulted in more scattered data points.

The initial thickness of the layers, h_i, is shown in figure 4 as a function of the lengthscale ξ, from 49 experiments conducted with salt, sugar and glycerol gradients. The range of ϕ_0 is 6×10^{-5}–6×10^{-3} (cm^{-1}) and the range of t_0 is 150–8000 s. The average ratio between h_i and ξ was 29 ± 3.8. This ratio is represented by the full line in the figure, the dashed lines represent the bounds of this average. This result, which is in good agreement with the one we deduced from the results of Chen *et al.* (1971) according to the discussion in §2.1, shows that the initial thickness of the layers depends on the ambient density gradient and fluid properties only. In figure 5 the non-dimensional initial thickness is plotted against the non-dimensional lengthscale $\delta_0/\xi = (K_T t_0)^{\frac{1}{2}}/\xi$, for the three different solutes. It is obvious that for the range of t_0 investigated there is no dependence of h_i on t_0. This is also an indication of the quasi-steady behaviour of the system for that range of t_0.

From figures 4 and 5 it is concluded that ξ is a proper lengthscale for the initial layers. Notice that the choice of K_S in ξ is an appropriate choice since there is no

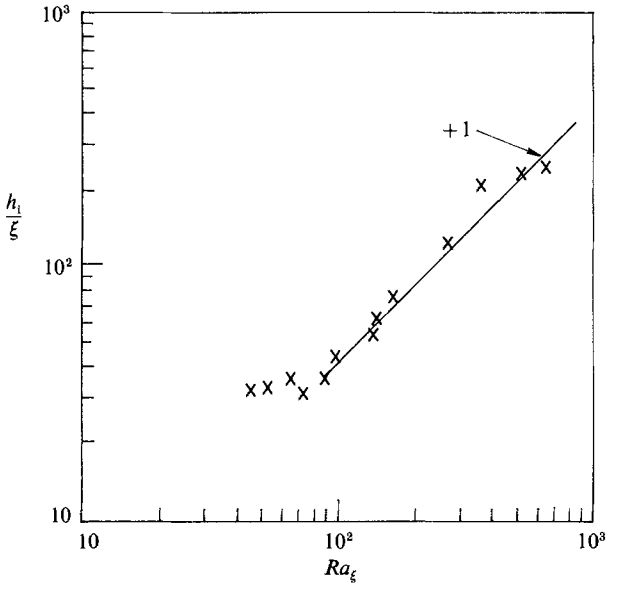

FIGURE 6. The dependence of the initial thickness of the layers on Ra_ξ for small t_0 (1.3–4 s).

deviation among the results for the three solutes. (K_S of sugar and glycerol is about $\frac{1}{3}K_S$ of salt). Recalling the result obtained by Thorpe *et al.* (1969) and by Hart (1971) that the initial cells rotate in alternating senses and immediately merge to form thicker cells, it is assumed that our initial thickness is twice the one resulting from the linear instability, which was not observed in our experiments owing to its very short lifetime.

The results from experiments with very rapid heating of the sidewall, corresponding to t_0 in the range 1.3–4 s, are shown in figure 6. For $35 < Ra_\xi < 70$ the initial thickness of the layers is independent of Ra_ξ and thus proportional to $\xi\,(\approx 30\xi)$, whereas for larger Ra_ξ, h_i/ξ is proportional to Ra_ξ, i.e. $h_i \propto \eta\,(= \alpha\Delta T/\phi_0)$ for $Ra_\xi > 70$ when the wall temperature is increased very fast. This is consistent with the results of Huppert & Turner (1980). One can see from their figure 4 that for $Ra_\eta < 2\times10^5 (Ra_\xi < 67)\, h/\eta \propto Ra_\eta^{-\frac{1}{4}}$, i.e. $h \propto \xi$, while for $Ra_\eta \geqslant 2\times10^5$, $h \propto \eta$. In non-dimensional terms rapid heating means that the time t_0 is much smaller than h_i^2/K_T ($\sim 10^2$ s in our experiments) while for slow heating t_0 is larger than h_i^2/K_T. The above-described behaviour seems also to be related to the first merging of the layers, which is discussed below.

4.2. *The merging process*

4.2.1. *Onset of first merging*

It was observed in our experiments that the layers that formed at the moment of instability persisted in their initial thickness up to the moment of first merging. To study this process a series of 20 experiments with salt and sugar was performed with the wall temperature (and Ra_ξ) increasing linearly with time. A typical plot of the non-dimensional instantaneous layer thickness as a function of the instantaneous Ra_ξ is in figure 7. It is seen that the initial thickness h_i/ξ, is maintained for some time although Ra_ξ is increased. At some $Ra_{\xi m}$ a rapid growth in the average thickness of

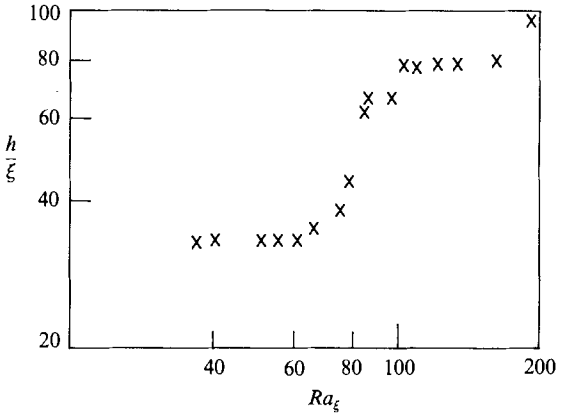

FIGURE 7. A typical plot of the instantaneous average layer thickness versus the instantaneous Ra_ξ illustrating the first merging.

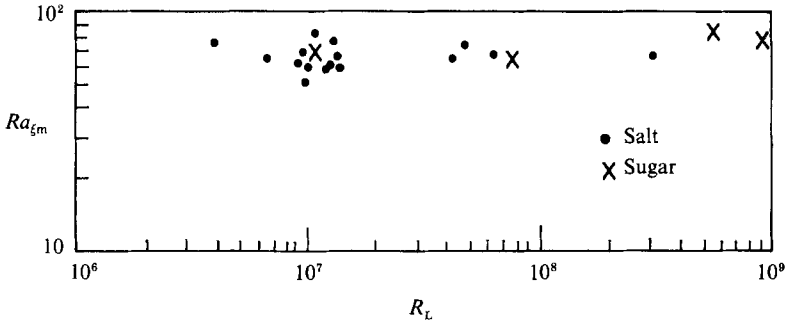

FIGURE 8. The criterion for onset of first merging, $Ra_{\xi m}$, as a function of R_L in experiments with a linear relation between wall temperature and time.

the layers occurs (the subscript m denotes state of merging). This growth is identified with the first merging.

The non-dimensional parameter representing the rate of temperature rise in experiments with linear heating is $R_L = [g/(\nu K_T)^{\frac{5}{2}}]^{\frac{1}{3}} \alpha c/\phi_0^3$, where c is the constant in the equation $\Delta T = ct$. In figure 8 $Ra_{\xi m}$ is plotted as a function of R_L, showing no dependence of the criterion for first merging on R_L. The value of $Ra_{\xi m}$ determined from 16 experiments appears to be equal to 66.4 ± 7.4. A similar result was obtained for sugar with slightly higher $Ra_{\xi m} = 75 \pm 6.8$ (4 experiments).

We also made observations (36 experiments with salt) of the first merging for the case when Ra_ξ (and the wall temperature) increased to a prescribed value following relation (1). These results are shown in figure 9 in which $Ra_{\xi m}$ is plotted as a function of the final Ra_ξ in each experiment. It is seen that when Ra_ξ is larger than ≈ 75 the first merging occurs at $Ra_{\xi m} = 75 \pm 8$, while when the final Ra_ξ is less than ≈ 75, first merging occurs at that Ra_ξ. The consequence of this result is that first merging always occurs although it was observed that for $Ra_\xi < 75$ it occurred after a longer time than for $Ra_\xi > 75$.

The existence of a criterion for the first merging suggests that this merging is due to subsequent instability of the system (following the formation of layers).

The criterion obtained above is comparable to the results obtained by Huppert &

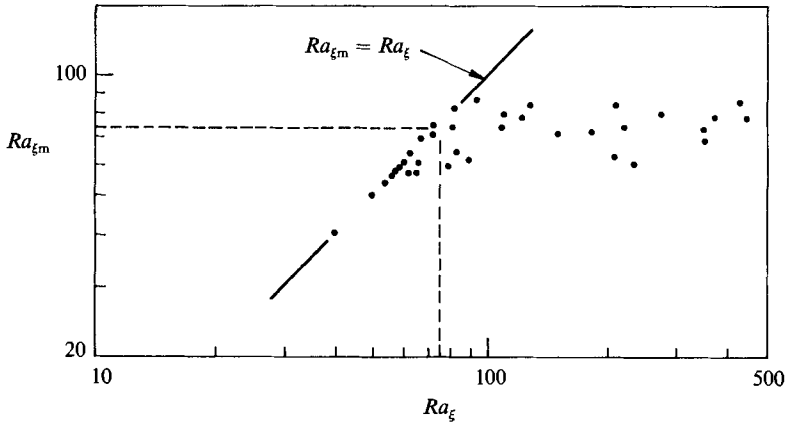

FIGURE 9. The criterion for onset of first merging, $Ra_{\xi m}$, as a function of the final Rayleigh number.

Turner (1980) and to our results from experiments with rapid heating (§4.1). As was shown in figure 6, for rapid-heating experiments initial layers are formed when $Ra_\xi < 67$ and layers of final thickness (proportional to η) are formed for $Ra_\xi > 67$. The agreement between this value of Ra_ξ and the value for $Ra_{\xi m}$ obtained above implies that in rapid-heating experiments with $Ra_\xi > Ra_{\xi m}$ the initial layers have a very short lifetime and they merge very fast to form final layers with thickness proportional to the imposed temperature difference ($h \propto \eta$).

4.2.2. *The subsequent merging process*

After the first merging, additional mergings generally occur until the layers attain their final thickness. We tried to obtain criteria for subsequent mergings, but soon it became apparent that no specific criteria could be obtained. The reason for this is discussed here on the basis of the results presented in figure 10. In this figure the non-dimensional instantaneous layer thickness, h/ξ, is plotted as a function of the instantaneous Rayleigh number, Ra_ξ, for five nearly identical experiments. The lines connecting the data points are drawn only to emphasize the distinction among the five sets of data. The five experiments were conducted with salt, with $\phi_0 = 0.0004$ cm^{-1}, $t_0 = 800$ s and a prescribed Rayleigh number, $Ra_\xi = 190$. The inset figure represents the rising curve of the wall temperature for the same five experiments according to relation (1) with $t_0 = 800$ s. In spite of the fact that all the physical parameters were the same, in each of the experiments a different pattern of the merging process was obtained. Furthermore, in the five experiments, the final Ra_ξ is about 190 and according to figure 13, which represents the dependence of h_f/h_i on Ra_ξ, for $Ra_\xi = 190, h_f/h_i = 4$. Indeed this ratio was obtained (± 0.2) in the five experiments but despite this 'regular' number ($h_f/h_i = 2^2$) the pattern of the merging process is different in each of the five experiments. Similar results were obtained for two other nearly identical experiments with $h_f/h_i = 6$. This result implies that after the first merging, which was regarded as a subsequent instability, the system of layers undergoes transition to chaotic behaviour. Since no specific criteria for subsequent mergings could be obtained, only a general aspect of the dynamics of the merging process was investigated and is presented in the following.

Two adjacent layers, separated by a density interface, may merge as a result of

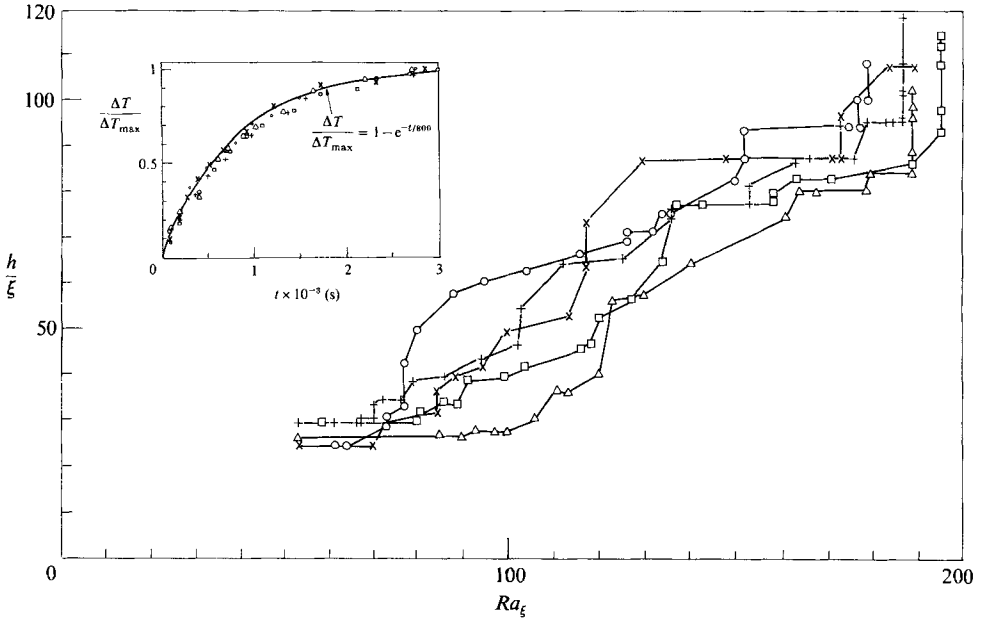

FIGURE 10. The instantaneous non-dimensional layer thickness h/ξ as a function of the instantaneous Ra_ξ in five, nearly identical experiments. In the inset figure the rising curve of the wall temperature in each of these experiments is shown (ΔT_{max} is the prescribed value of ΔT).

equalization of densities below and above that interface. In our case the interface is of 'diffusive' type, i.e. saltier and hotter fluid lies underneath less salty and colder fluid. The non-dimensional density jump at the interface due to temperature is $\Delta\rho_T/\rho_0 = \alpha\Delta T_v$, where ρ_0 is a reference density and ΔT_v is the temperature difference across the interface which may be expressed as $\Delta T_v = A_T\Delta T$, where A_T is a coefficient and ΔT is the horizontal overall temperature difference. The non-dimensional density jump at the interface due to salinity is $\Delta\rho_S/\rho_0 = \beta\Delta S$, where ΔS is the salinity jump at the interface. If we asume that the layers are of equal thickness h and are well mixed we can substitute $\Delta S = -h\,\mathrm{d}s_0/\mathrm{d}z$ and obtain $\Delta\rho_S/\rho_0 = -\beta h\,\mathrm{d}s_0/\mathrm{d}z = A_S\xi\phi_0$, where $A_S = h/\xi$. If the merging of the two layers is due to the equalization of their densities, a general condition for merging is $A_T\alpha\Delta T \geqslant A_S\xi\phi_0$. Rearranging this relation we obtain

$$Ra_\xi \geqslant A_S/A_T. \tag{10}$$

In order to check the validity of this condition, A_S and A_T should be determined at different stages of layers merging during an experiment. A_S is equal to the instantaneous h/ξ, and A_T can be extracted from temperature measurements across an interface. We had carried out such measurements during the merging process in two typical experiments and obtained from 17 temperature profiles the ratio $Ra_\xi/(A_S/A_T) = 0.48 \pm 0.08$.

The quantitative disagreement between this result and (10) suggests that merging of two adjacent layers in our experiments is not a result of reduction in density differences only and that there are some other mechanisms contributing to that process. These mechanisms are assumed to be: (i) the conversion of kinetic energy of the fluid convecting inside the layers into potential energy; and (ii) the diffusive

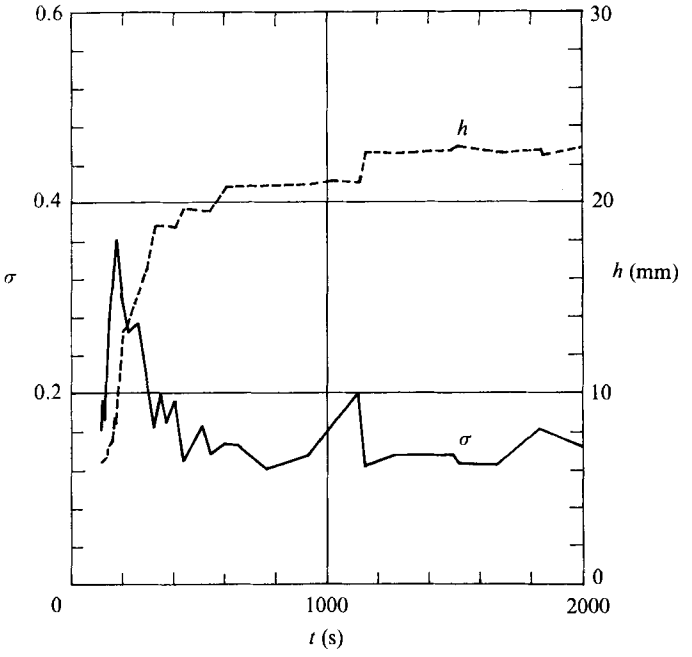

FIGURE 11. The average thickness of the layers, h, and its standard deviation, σ, as a function of time in a typical experiment.

transport of salt across the interface which was not taken into account in the derivation of (10). (This effect seems to be minor owing to the continuous supply of salt from the far stratified fluid.)

A crude estimation that we performed showed that the potential energy needed to equalize the densities below and above an interface just before merging takes place is of the same order of magnitude as the kinetic energy of the fluid inside the layer.

It should be pointed out here that the result that kinetic energy contributes to the merging of layers is different from the result by Huppert & Linden (1979) who showed that merging of layers produced by heating a stable salinity gradient from below is primarily due to equalization of densities. This point will be discussed in §4.4.3.

Since, during the merging process, some layers increase their thickness at the expense of other layers whose thickness is decreased, large non-uniformities in the thickness of the individual layers are expected especially at the stage of merging. A measure for these non-uniformities is the standard deviation from the average layer thickness. In figure 11, the average thickness of the layers, h, and the standard deviation, σ, are plotted as a function of time for a typical experiment. It is seen that almost every stage of merging, which is characterized by a sharp growth in h, is associated with a local maximum in σ as expected.

4.3. *The final thickness of the layers*

The final thickness of the layers was defined as the thickness the layers attained after the temperature difference reached its prescribed value. It should be pointed out that this thickness persisted until the layer fronts almost reached the opposite wall of the

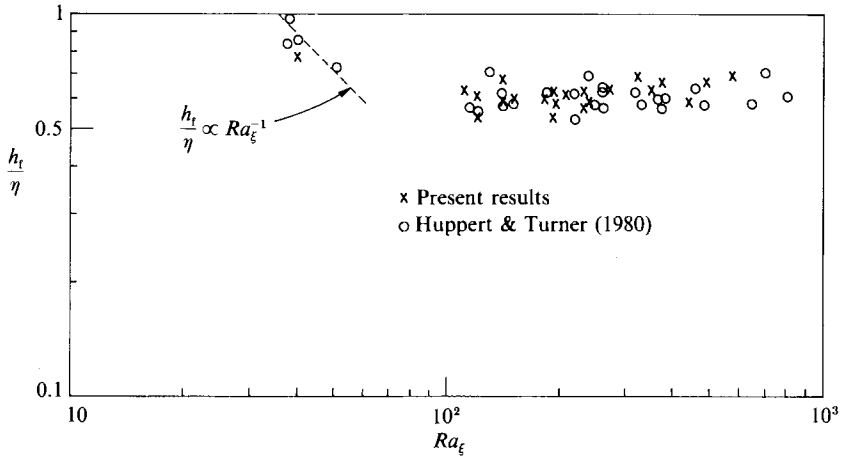

FIGURE 12. The dependence of the non-dimensional final thickness of the layers, h_f/η, on the final Rayleigh number.

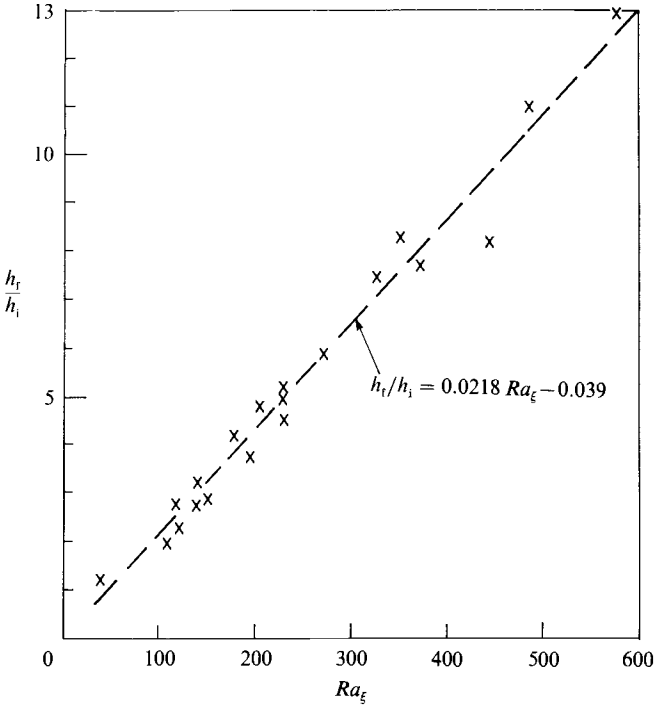

FIGURE 13. The ratio between the final and the initial thickness of the layers, h_f/h_i, as a function of the final Rayleigh number.

tank (120 cm wide). In figure 12 the non-dimensional final thickness of the layers, h_f/η, is plotted as a function of the final Ra_ξ from experiments conducted in the large tank with salt gradients only. Except for the result at $Ra_\xi = 40$, h_f/η does not depend on Ra_ξ and has a constant average value of $h_f/\eta = 0.62 \pm 0.1$. For comparison, the results obtained by Huppert & Turner (1980) are also shown in this figure. A very good agreement is found to exist between the two sets of data. From this it is

concluded that the lengthscale η is a proper lengthscale for the final layers provided $Ra_\xi > 70$. For $Ra_\xi < 70$, the results of Huppert & Turner (1980) and our single result at $Ra_\xi = 40$ give the ratio $h_f/\eta \propto Ra_\xi^{-1}$. Rearranging this one obtains $h_f \propto \xi$ which implies that for $Ra_\xi < 70$ initial layers are formed. This result is related to the first merging of the layers as was discussed earlier.

It was suggested in §2.2 that the ratio between the final and the initial thickness of the layers depends on Ra_ξ and thus can assume any positive number greater than unity. This dependence is shown in figure 13 where h_f/h_i is plotted as a function of the final Ra_ξ. The straight dashed line represents the equation

$$h_f/h_i = 0.0218 Ra_\xi - 0.039,$$

which is in good agreement with the ratio predicted in §2.2 (equation (6)). The consequence of that result is that the merging process of the layers in these experiments is not a simple successive doubling of the layers thickness, a result which is entirely different from that of Wirtz & Reddy (1979) for the case of the narrow slot. Since they investigated a different physical configuration, it is reasonable to assume a different behaviour of the system of layers.

4.4. *The structure of the layers and the interfaces*

The structure of the layers in different stages of their development was studied by two visualization techniques, namely fluorescent dye and fluorescent particles.

4.4.1. *The initial layers*

A typical set of photographs, showing the initial layers and their subsequent development is in figure 1. The initial layers (1*a*) consist of roll-cells of equal size. These cells are the immediate result of vorticity production at the wall owing to the horizontal temperature and salinity gradients. The cells slope slightly down with the distance from the wall owing to the decrease in temperature in that direction. It is noteworthy that all cells rotate in the same sense and alternating rotation, as discussed by Thorpe *et al.* (1969) and by Hart (1971), is not observed in our experiments.

Particles-trace photographs of the initial cells (figure 14*a*) show that they are separated by thin regions in which only horizontal flow exists. These regions are identified with the interfaces between the layers. It is seen that the horizontal flow at the interfaces spreads laterally beyond the fronts of the cells, an observation that implies the existence of shear flow in the ambient far fluid. This shear flow is discussed in more detail later.

4.4.2. *The merging process*

The two mechanisms of merging described by Linden (1976), namely interface breakdown and interface migration, were observed in our experiments too. It should be pointed out that in our two-dimensional observations (in contrast to Linden 1976), merging always started near the heated wall according to one of the mechanisms mentioned above and then propagated gradually through the body of the two layers, eventually completing their merging.

In figure 15 an inclined interface is seen. This situation is the result of vertical migration of the interface near the wall. The inclined part of the interface moves gradually from the wall as seen in figure 15. At this stage the average thickness of the layers depends on the distance from the wall but since, in this work, we always related the instantaneous average layer thickness to the instantaneous temperature

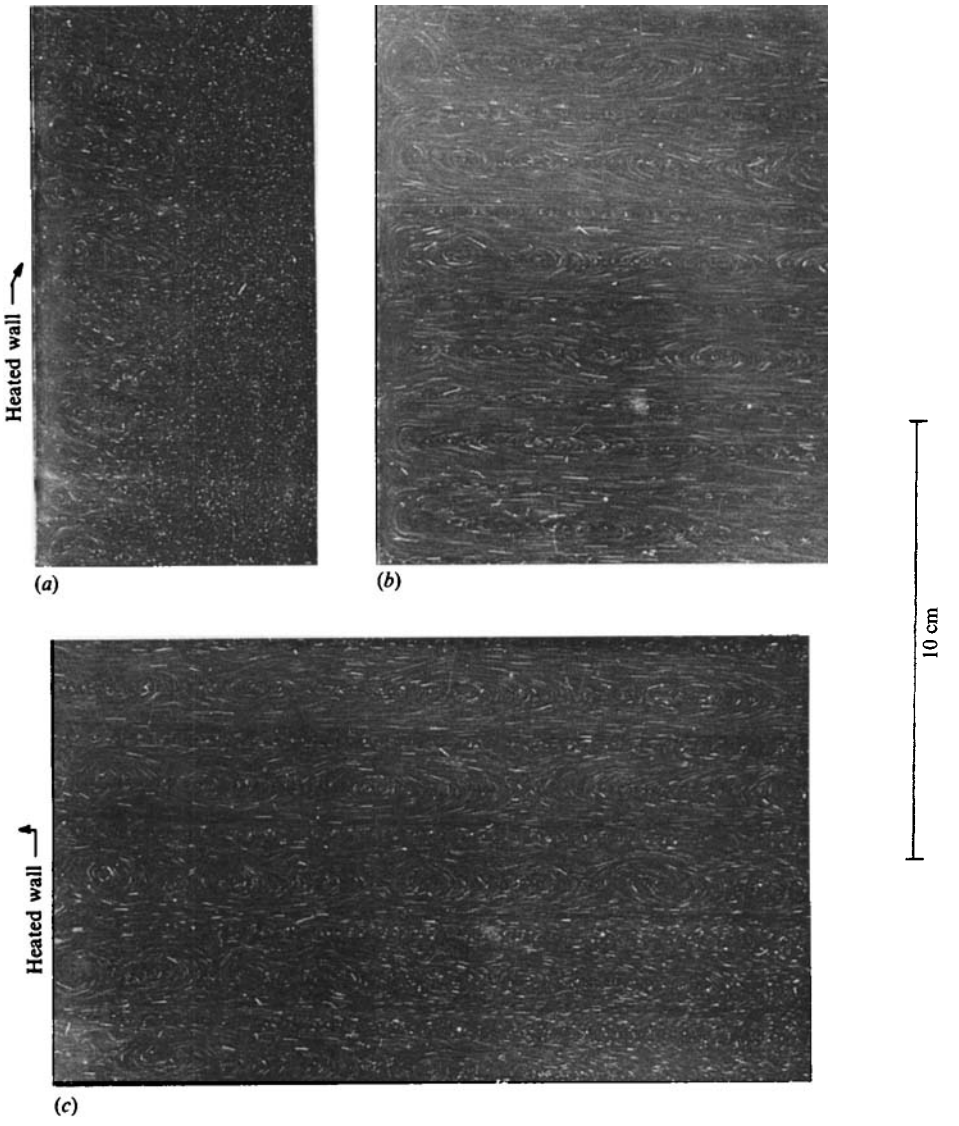

FIGURE 14. Fluorescent-particle flow visualization of the layers. (*a*) initial layers; (*b*) developed layers near the heated wall; (*c*) developed layers (fragment).

at the wall, two layers were said to be already merged just after their merging started at the wall. Merging due to breakdown of an interface is shown in figure 16. Here, the interface was broken down near the wall, causing partial mixing between the layers, and a front-like interface was formed. As shown in the successive photographs, the mixed region grows laterally with time, eventually completing the merging of the two layers.

The observations described above are in agreement with the 'wavy-like' interface observed by Turner & Chen (1974) in their two-dimensional experiments and with Tsinober *et al.* (1983) who studied the flow due to a point source of heat in a stable salinity gradient (see their figure 6). This general agreement suggests that these

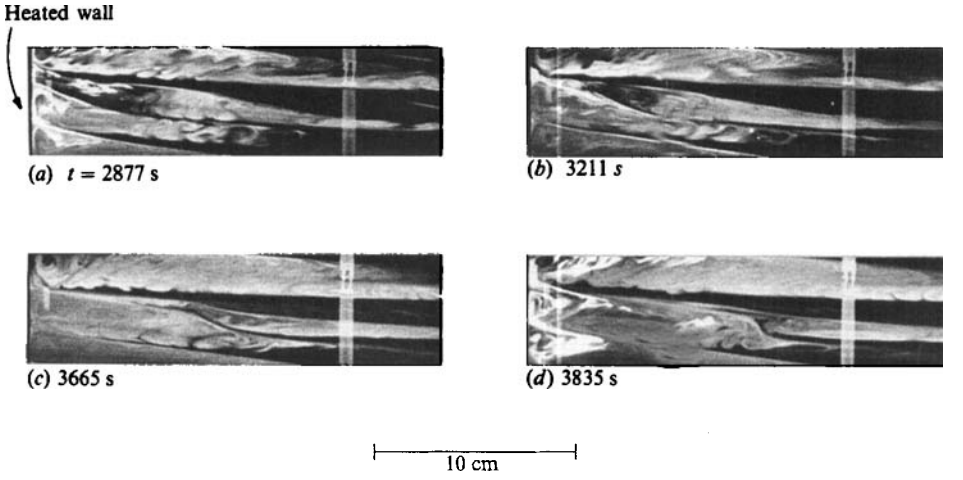

FIGURE 15. Merging of two layers separated by an inclined interface formed as a result of vertical migration close to the heated wall.

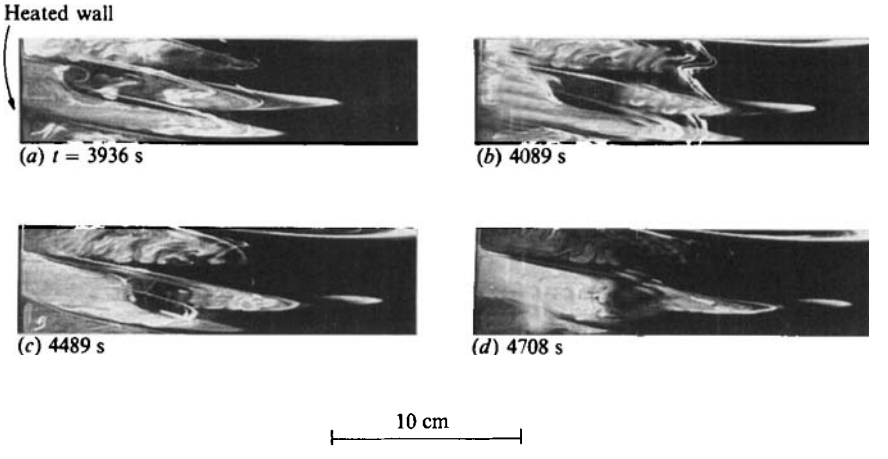

FIGURE 16. Merging of two layers with a front-like interface which is formed owing to partial breakdown of the interface separating the layers.

phenomena are typical of double-diffusive convection with horizontal gradients of the two buoyancy components.

The preference of one of the merging mechanisms over the other seemed, in our observations, to be somewhat random, in agreement with the chaotic nature of the merging process discussed earlier. However, it is probable that a more detailed investigation, including temperature, salinity and velocity measurements within the layers, can lead to some more conclusive results. Such measurements were outside the scope of this work.

4.4.3. *The developed layers and interfaces*

The particles-trace photographs in figure 14 indicate that the developed layers consist of vortices with a vertical scale of the layer thickness. There is not a single

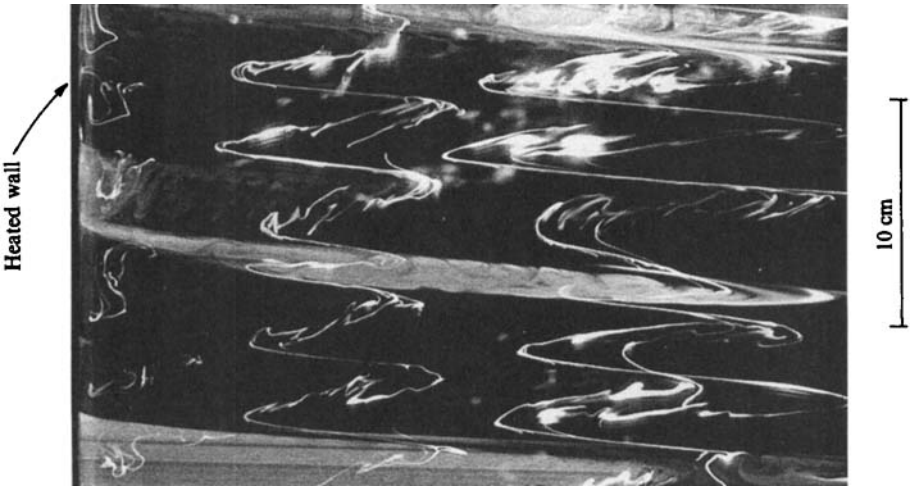

FIGURE 17. Fluorescent dye traces showing the stable shear flow at the interfaces (almost horizontal straight lines) and the unstable shear flow within the layers (inclined convoluted lines).

horizontal scale of these vortices and in figure 14(*b*) we observe very large vortices in the two layers at the bottom and some vortices of smaller horizontal scale in the two layers at the top of the picture. (This picture is a fragment and the top and bottom layers shown are not close to the horizontal boundaries of the tank.) Similar diversity of horizontal scales is observed in figure 14(*c*). The vortices in each layer are bounded from top and bottom by relatively thin regions in which only horizontal motions exist. Each of these regions is subdivided by an even thinner region where the velocity is almost zero. This region is identified with the core of the interface across which all transport takes place by molecular diffusion only. The motion on top of the interface is towards the hot wall (at the left) and that below the interface is in the opposite direction, and thus a parallel shearing motion is produced.

The observed vortices seems to be produced and maintained by two vorticity-generating mechanisms. The first is the quasi-horizontal shear flow described above and the second results from the horizontal gradients of solute concentration and temperature which are significant mainly close to the wall and, in fact, are the primary source of double-diffusive instability.

It is also suggested that the vortices, which are typical of two-dimensional double-diffusive convection (Tsinober, Yahalom & Shlien 1983), play an important role in the merging of layers since these vortices contain most of the kinetic energy of the flow inside the layers. This may also imply an essential difference between one-dimensional situations in which, as Huppert & Linden (1979) showed, merging is primarily due to density equalization and the present two-dimensional case where equalization of densities was found to be unnecessary for merging to occur (see §4.2.2).

It is obvious from the photographs that the parallel shear flow at the interface is stable while the shear flow inside the body of the layers is unstable, giving rise to the production of the vortices. This behaviour is vividly demonstrated by the photograph in figure 17. This picture was produced by dropping particles of fluorescent dye at different horizontal locations far from the wall. The lines of dye that were vertical initially, are deformed by the flow, thus illustrating the velocity

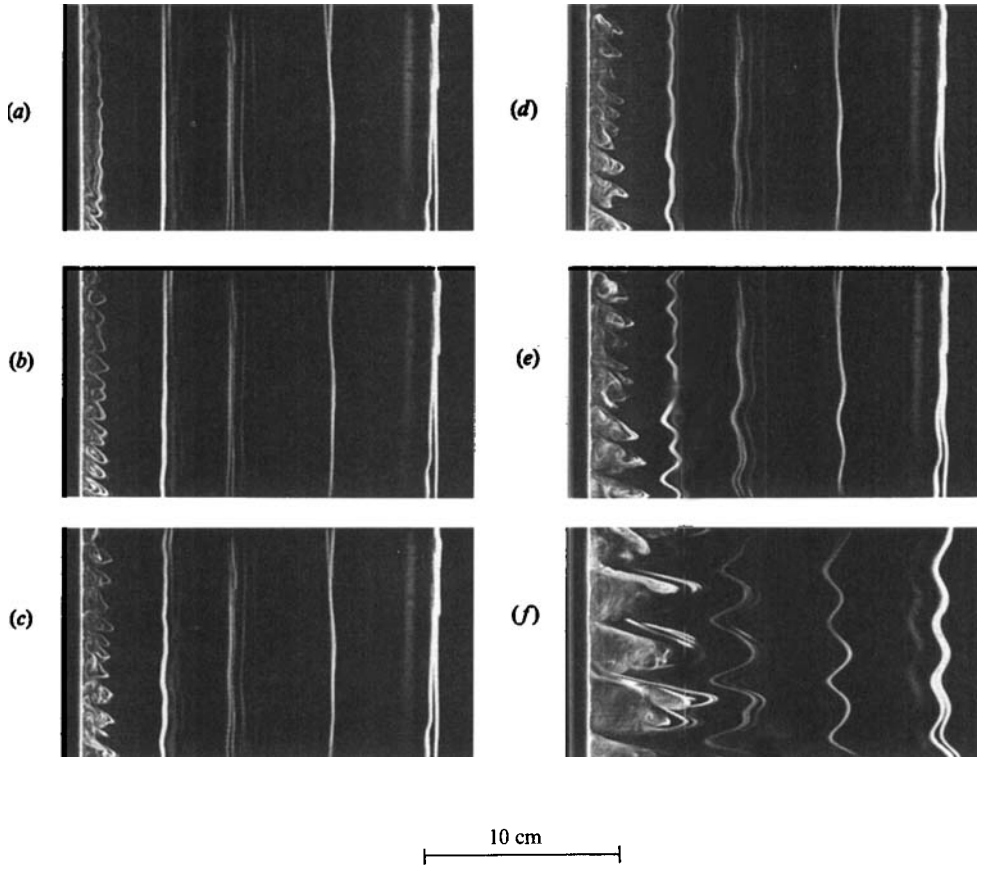

FIGURE 18. Fluorescent dye traces illustrating the formation and development of horizontal shearing motion in the ambient fluid.

profile in the layers and at the interfaces. The stable shear flow at the interfaces is represented by the straight almost horizontal lines of dye while the unstable shear flow within the layers is represented by the inclined convoluted lines of dye.

4.4.4. *Shearing motion in the ambient fluid*

It was observed in §4.4.1 that the horizontal flow at the interfaces separating the initial cells, spread laterally into the ambient fluid beyond the mixed regions of the cells themselves. This phenomenon was investigated in more detail by dropping particles of fluorescent dye in the interior of the quiescent fluid before initiation of heating. The resulted deformation of these lines of dye after initiating the heating of the wall is shown in the sequence of photographs in figure 18. In figure 18(*a*), initial layers are just formed at the heated wall on the left and the vertical lines of dye are still straight. In the following pictures the successive deformation of the lines is observed, indicating the existence of internal waves that propagate horizontally much faster than the layer fronts (similar waves were observed by Turner 1978). The deformed lines do not exhibit any mixing (the lines are not convoluted) and only stable horizontal parallel shear flow seems to exist.

5. Concluding remarks

An experimental investigation has been performed which considers a linear stable solute gradient destabilized by heating from one sidewall in a wide tank.

The results show that the stability diagram of the system in the phase plane is similar to that of a linear solute gradient heated differentially in a vertical narrow slot. The diagram obtained exhibits transition from shear to double-diffusive instability, and reveals the destabilizing effect of the solute gradient at small values of Ra_S (≈ 10).

The criterion for the onset of layers, obtained from the stability diagram, and the initial thickness of the layers, are both independent of the time history of the wall temperature and are defined by the undisturbed density gradient and fluid properties. The only exception from this conclusion is the case of almost impulsive heating of the wall. Here, for Ra_ξ larger than $Ra_{\xi m}$ (the critical value for the first merging) layers of thickness proportional to η (i.e. final layers) are formed at the onset of instability while for $Ra_\xi < Ra_{\xi m}$ initial layers of thickness proportional to ξ are formed.

After the onset of layers, as the temperature of the wall further increases, the initial layers start to merge. A criterion for the first merging is obtained and the observations show that after the first merging the system of layers undergoes transition to chaotic behaviour. This was concluded from the result that in each of five nearly identical experiments the subsequent merging process exhibited different behaviour. It is thus concluded that the system of layers in the stages of subsequent mergings is very sensitive to small perturbations in the boundary and/or initial conditions.

In spite of the chaotic behaviour of the system of layers during the subsequent merging process, the final thickness of the layers is always proportional to the prescribed lateral temperature difference.

Flow-visualization experiments show that quasi-horizontal shearing motion in the far fluid is induced by the layers. This motion suggests the existence of internal waves which are produced at the moment of layer formation and propagate laterally much faster than the layer fronts.

We would like to acknowledge very useful discussions with Professor J. S. Turner at the initial stages of this research (§§4.1, 4.2.1). We are also grateful to our referees whose comments aided the improvement of the manuscript.

REFERENCES

CHEN, C. F., BRIGGS, D. G. & WIRTZ, R. A. 1971 Stability of thermal convection in a salinity gradient due to lateral heating. *Intl J. Heat Mass Transfer* **14**, 57–65.

HART, J. E. 1971 On sideways diffusive instability. *J. Fluid Mech.* **49**, 279–288.

HART, J. E. 1973 Finite amplitude sideways diffusive convection. *J. Fluid Mech.* **59**, 47–64.

HUPPERT, H. E., KERR, R. C. & HALLWORTH, M. A. 1984 Heating or cooling a stable compositional gradient from the side. *Intl J. Heat Mass Transfer* **27**, 1395–1401.

HUPPERT, H. E. & LINDEN, P. F. 1979 On heating a stable salinity gradient from below. *J. Fluid Mech.* **95**, 431–464.

HUPPERT, H. E. & TURNER, J. S. 1980 Ice blocks melting into a salinity gradient. *J. Fluid Mech.* **100**, 367–384.

HUPPERT, H. E. & TURNER, J. S. 1981 Double-diffusive convection. *J. Fluid Mech.* **106**, 299–329.

LINDEN, P. F. 1976 The formation and destruction of fine-structure by double diffusive process. *Deep-Sea Res.* **23**, 895–908.

NARUSAWA, U. & SUZUKAWA, Y. 1981 Experimental study of double-diffusive cellular convection due to a uniform lateral heat flux. *J. Fluid Mech.* **113**, 387–405.

PALIWAL, R. C. & CHEN, C. F. 1980 Double-diffusive instability in an inclined fluid layer. Part 2. Stability analysis. *J. Fluid Mech.* **98**, 769–785.

SUZUKAWA, Y. & NARUSAWA, U. 1982 Structure of growing double diffusive convection cells. *Trans. ASME* C: *J. Heat Transfer* **104**, 248–254.

TANNY, J. & TSINOBER, A. B. 1987 On the merging of double diffusive layers. In *Proc. 3rd Intl Symp. on stratified flows, CIT, California.*

THANGAM, S., ZEBIB, A. & CHEN, C. F. 1981 Transition from shear to sideways diffusive instability in a vertical slot. *J. Fluid Mech.* **112**, 151–160.

THORPE, S. A., HUTT, P. K. & SOULSBY, R. 1969 The effect of horizontal gradients on thermohaline convection. *J. Fluid Mech.* **38**, 375–400.

TSINOBER, A. B. & TANNY, J. 1985 On the structure and dynamics of double diffusive layers in sidewall heating experiments. In *Double Diffusive Motions* (ed. N. E. Bixler & E. Speigel), FED-vol. 24, pp. 39–45. ASME.

TSINOBER, A. B. & TANNY, J. 1986 Visualization of double diffusive layers. In *Flow Visualization IV* (ed. Claude Veret), pp. 345–351. Hemisphere.

TSINOBER, A. B., YAHALOM, Y. & SHLIEN, D. J. 1983 A point source of heat in a stable salinity gradient. *J. Fluid Mech.* **135**, 199–217.

TURNER, J. S. 1974 Double diffusive phenomena. *A. Rev. Fluid Mech.* **6**, 37–56.

TURNER, J. S. 1978 Double-diffusive intrusion into a density gradient. *J. Geophys. Res.* **83**, 2887–2901.

TURNER, J. S. 1979 Laboratory models of double diffusive processes in ocean. In *Proc. 12th Symp. Naval Hydr., Washington D.C.*, pp. 596–606.

TURNER, J. S. 1985 Multicomponent convection. *Ann. Rev. Fluid Mech.* **17**, 11–44.

TURNER, J. S. & CHEN, C. F. 1974 Two dimensional effects in double diffusive convection. *J. Fluid Mech.* **63**, 577–592.

WIRTZ, R. A., BRIGGS, D. G. & CHEN, C. F. 1972 Physical and numerical experiments on layered convection in a density-stratified fluid. *Geophys. Fluid Dyn.* **3**, 265–288.

WIRTZ, R. A. & REDDY, C. S. 1979 Experiments on convective layer formation and merging in a differentially heated slot. *J. Fluid Mech.* **91**, 451–464.